



# Power deposition measurements in deuterium and helium discharges in JET MKIIGB divertor by IR-thermography

T. Eich <sup>a,\*</sup>, A. Herrmann <sup>a</sup>, P. Andrew <sup>b</sup>, A. Loarte <sup>c</sup>,  
Contributors to the EFDA-JET Program

<sup>a</sup> Max-Planck-Institut für Plasmaphysik, Association EURATOM-IPP, Boltzmannstraße 2, 85748 Garching, Germany

<sup>b</sup> EURATOM-UKAEA Fusion Association, Culham Science Centre, Abingdon, Oxfordshire OX14 3EA, UK

<sup>c</sup> CSU-EFDA, Max-Planck-Institut für Plasmaphysik, 85748 Garching, Germany

Received 27 May 2002; accepted 12 September 2002

---

## Abstract

One of the outstanding problems for a next step fusion device is the handling of the power fluxes into the divertor, in particular regarding fast transient heat deposition by edge localised modes (ELMs). For a next step fusion device, such as ITER, type-I ELMy H-Mode is the reference discharge and therefore of particular interest. At JET a thermography system with high time resolution is able to resolve temperature evolution during and between ELM periods; here, the analysis is focussed so far on type-I ELMy H-Mode discharges with ELM frequencies of 10–35 Hz. Influences from surface layers on the target tiles are investigated in special discharges and taken into account. Results about the distribution of ELM and inter-ELM power deposition on the inner and outer divertor target plates are presented. Additionally, the characteristic ELM power deposition time (or temperature rise time) and its dependence on pedestal parameters are studied. The thermal impact due to ELMs for ITER is calculated together with predictions for relative ELM midplane losses and heat flux evolution on the divertor target. The predicted values based on conservative assumptions exceed the material limits.

© 2003 Elsevier Science B.V. All rights reserved.

PACS: 52.40.Hf

Keywords: JET; Divertor; ELMs; Power deposition measurements; IR-thermography; ITER

---

## 1. Temperature measurements and heat flux calculations

The 2D IR-system on JET is equipped with a periscope optic for viewing the ITER like MKIIGB gas box divertor. The IR-Camera is sensitive to photons in the wavelength range from 3 to 5  $\mu\text{m}$ , which allows the calculation of the divertor surface temperatures assuming Planck's law for black body radiation (and neglect-

ing further radiation for instance by molecules or ablated carbon during edge localised modes (ELMs)) with a time resolution of up to 21  $\mu\text{s}$ . A set of ELMy H-Mode discharges with an IR-optimised strike zone position have been performed. The transformation procedure developed to interpret the periscope view was used to deduce poloidal profiles of the temperature distribution on the target tiles [1].

Significant differences between the temperature evolution of the target surface in the inner and outer divertor chamber (split by the septum of MKIIGB) were observed in deuterium discharges. The temperature at the inner leg evolves step like with heating power,

---

\* Corresponding author. Tel.: +49-89 3299 1927; fax: +49-89 3299 2580.

E-mail address: [thomas.eich@ipp.mpg.de](mailto:thomas.eich@ipp.mpg.de) (T. Eich).

Table 1

Energy distribution for two H-Mode discharges derived by IR-measurements. The derived values by thermocouples measurements (TC) are shown for comparison

#53764				#53765			
Inner (tile #3)		Outer (tile #7)		Inner (tile #3)		Outer (tile #7)	
21 MJ (TC: 16 MJ)		31 MJ (TC: 33 MJ)		27 MJ (TC: 24 MJ)		80 MJ (TC: 80 MJ)	
Inter	ELM	Inter	ELM	Inter	ELM	Inter	ELM
ELM		ELM		ELM		ELM	
12 MJ	9 MJ	21 MJ	10 MJ	7 MJ	20 MJ	55 MJ	25 MJ

whereas an increase with the square root of time was found in the outer leg. Such effects, attributed to a change of the surface properties, have been already reported from ASDEX Upgrade [2] and JET [3]. For discharges in helium ( $\sim 40$  discharges have been run between the observed changes) the behaviour of the measured surface temperature for the inner divertor changes and becomes equal to the behaviour of the surface temperature on the outer target tiles [5].

A method to calculate the heat flux deposition from the temperature evolution including these surface layers is the introduction of a heat transmission coefficient in the heat flux calculation as done with the THEODOR code [4]. The deposited energy calculated with this method and that derived by thermocouple measurements are in good agreement [5]. The global balance between input, deposited and radiated energy is matched within error bars of 10–20% for H-Modes at high  $P_{\text{heat}}$ . In low powered L-Mode discharges this discrepancy is up 40%, because the background signal from the periscope optics is in the same range as the signal for low temperatures (80–200°).

## 2. Energy distribution onto the inner and outer target plates in H-mode discharges

To distinguish between energy deposition during and in between ELMs two methods are used. First, a pulse height analysis is performed, in which the power deposition per time interval (which is the frame rate of the 2D camera array and corresponds to roughly 2 ms) is integrated and ordered due to corresponding energy.

Another method cuts the higher power deposition during ELMs by defining a start time and end time around the ELM event integrating the power in that time window. Here it should be noted, that the end of the ELM power deposition is difficult to define because it varies in dependence of heat transmission coefficient used for the heat flux calculation. However, due to the reduced heat flux after the ELM for roughly 10–30 ms for type-I ELMs with frequencies in the range of 10–35 Hz, the error by choosing various end times for the ELM power deposition interval stays small. Nevertheless, both applied methods come to similar values and

are combined to deduce the power distribution in ELMy H-Mode discharges.

In Table 1, the distribution of energy in the two type-I ELMy H-Mode discharges is shown (#53764,  $P_{\text{NBI}} = 9$  MW,  $n_{\text{av}} = 4 \times 10^{19} \text{ m}^{-3}$  and #53765,  $P_{\text{NBI}} = 16$  MW,  $n_{\text{av}} = 6 \times 10^{19} \text{ m}^{-3}$ ). In pulse #53764 both the inner and the outer divertor are attached, whereas in pulse #53765 the inner divertor is partly power detached. The energy deposition due to the type-I ELMs in both discharges is fairly balanced, whereas the inter-ELM energy deposition is dominated by the outer divertor (almost completely if the inner divertor is highly detached). The balanced energy deposition during ELMs found by thermography and calorimetry (TC) [6] is close to DIII-D [7] but appears somewhat different from results reported from ASDEX-Upgrade, where an in/out ratio of 2/1 (or even higher values favouring the inner target) is found during ELMs [8].

## 3. ELM power deposition times on the divertor target

An important aspect of the mechanism that governs the power deposition onto the target plates and its consequences for a next step fusion device like ITER is the characteristic time of SOL energy transport by ELMs. The time of the largest temperature rise on the outer target during reproducible type-I ELMs are compared with the pedestal plasma parameters just before the ELM event occurs. For the analysis presented here, investigations have been mainly focussed on the outer divertor, because the view in the inner divertor is much more restricted. Nevertheless, for some discharges a comparison of inner and outer target was performed and lead to the same conclusions concerning the characteristic behaviour for ELM target load reported here.

In Fig. 1, the evolution of the heat flux profile on the outer divertor target is shown for #53765 prior to and during the ELM event. The position of the heat flux maximum and the profile shape are not changed significantly. The maximum heat flux reaches a value of  $90 \text{ MW m}^{-2}$ . Here, to reduce the data scatter, about 7 ELMs (corresponding to 22.5–23.0 s in #53765) during

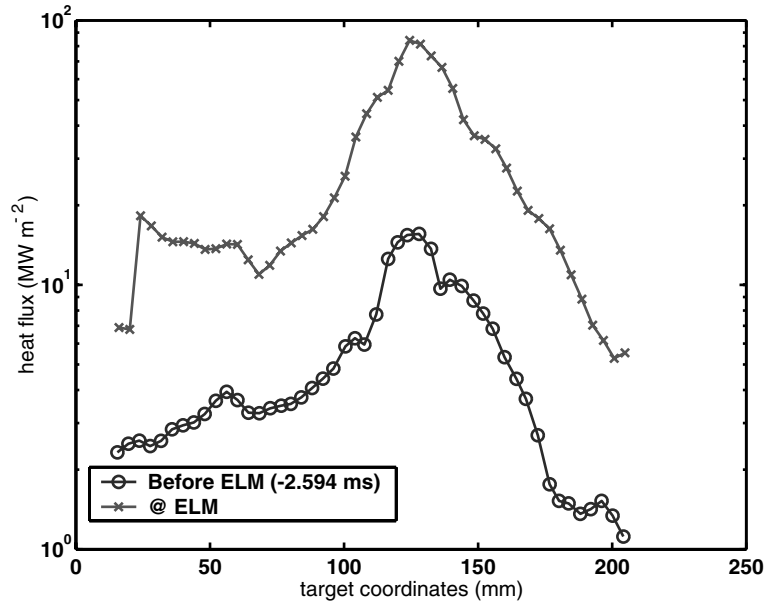


Fig. 1. The heat flux profile on the outer target before and during the maximum heat flux of an averaged ELM event (22.5–23.0 s in #53765, 7 ELMs). The profile shape is not changed significantly and the position of the heat flux maximum is not shifted more than a few mm compared to in between ELM values.

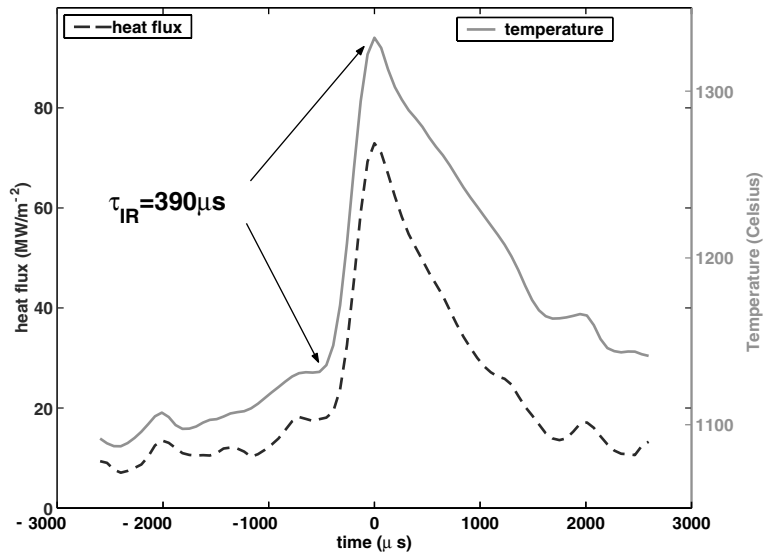


Fig. 2. The maximum of the temperature and the heat flux density for an averaged ELM (19.5–20.0 s in #53767, 17 ELMs). The ELM rise time derived by the fast temperature (or heat flux) rise is 390  $\mu\text{s}$  on the outer target, the small increase of temperature and heat flux prior to the ELM is not taken into account.

the flat top phase are averaged to one ELM (by synchronizing the time signal in respect to the peak value of the power deposition of each single ELM). In Fig. 2 the maximum of the temperature and heat

flux evolution for an averaged ELM (17 ELMs corresponding to 19.5–20.0 s in #53767) is presented. The time, in which the temperature (or heat flux) rises from the inter-ELM value to the maximum heat flux

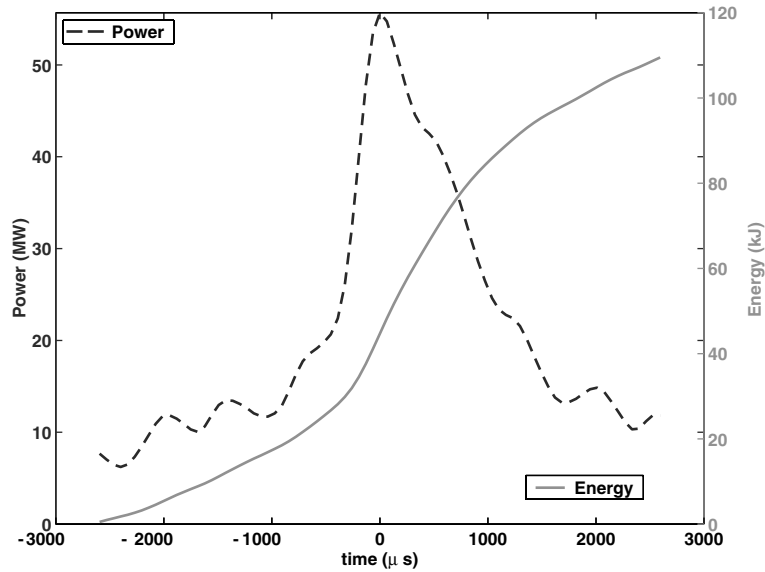


Fig. 3. The power and the integrated energy of an averaged ELM (19.5–20.0 s in #53767, 17 ELMs) for the outer divertor target tile.

during the ELM event is taken as a characteristic time for the ELM power deposition (named  $\tau_{\text{IR}}$ ) and used for the extrapolation to ITER in Section 4. Furthermore, the deposited power and integrated energy during the (averaged) ELM event are shown in Fig. 3. Here, the triangular shape of the temporal power evolution should be noted (in contrast to a uniform rectangular shape with constant heat flux) for the discussion in Section 4.

It should be noted, that the described averaging method is only possible for the so called IR-optimised discharges due to the combination of the complex viewing geometry, the strike zone positioning and the desired data acquisition with highest frequencies and was therefore only performed for a subset of discharges at JET. For a much higher number of discharges the temperature rise time has been taken as the ELM rise time without performing heat flux calculation or ELM averaging.

The small temperature rise prior to the ELM is not taken into account in the ELM rise time, because (a) the high noise level does not allow a reasonable quantification of the start time and (b) the slight increase compared to steep gradient prior to the maximum is very small.

In Fig. 4, the correlation of the ELM rise time ( $\tau_{\text{IR}}$ ) for various plasma conditions with the parallel ion transport time defined by the ion sound speed and the connection length ( $\tau_{\parallel} = L_{\text{C}}/c_{\text{s}}$ ) is shown. Here, the connection length is taken as  $L_{\text{C}} = 2\pi R q_{95}$ . Furthermore, it is assumed that  $T_{\text{i}}$  equals  $T_{\text{e}}$  in the pedestal region (origin of the ELM power release) and that  $T_{\text{e}}$  is a reasonable value to calculate the collisionless iso-

thermal (ballistic) sound speed of the ions. Typically, the parallel ion transport time in JET ranges from 100 to 250  $\mu\text{s}$  and corresponding type-I ELM power deposition times in a range of 100–550  $\mu\text{s}$ . Measurements in the JET MKIIa divertor [10] which reported ELM power deposition times of 100  $\mu\text{s}$  were from discharges at high  $I_{\text{p}}$  with pedestal temperatures  $>2.5$  keV and, hence, short  $\tau_{\parallel}$ .

#### 4. Extrapolation of the type-I ELM power fluxes to ITER

Multi-machine parametrisation for the relative ELM losses predict values around 10–15 MJ for ITER in the expected edge collisionality range and a corresponding parallel ion transport time of 240  $\mu\text{s}$  in the SOL [9]. The maximum target heat load for ITER can be derived assuming the above mentioned deposition time and the same temporal evolution of the ELM heat flux as found in JET MKII GB (as well as on ASDEX Upgrade [8]). Here, it should be noted that only a fraction of the target load energy arrives during the defined ELM power deposition time, whereas some more power arrives in the tail after the maximum heat flux. Again, due to the influence of surface layers the fraction of the energy deposited during the rise of the peak heat flux and its decline can only be given within certain limits. Nevertheless, it is reasonable to assume that a similar energy flow occurs before and after the peak heat flux (although the heat flux measurements in Fig. 2 indicate even critical values). Further information about the heat flux profile and the relative size of the ELM power deposition compared to mid plane losses has

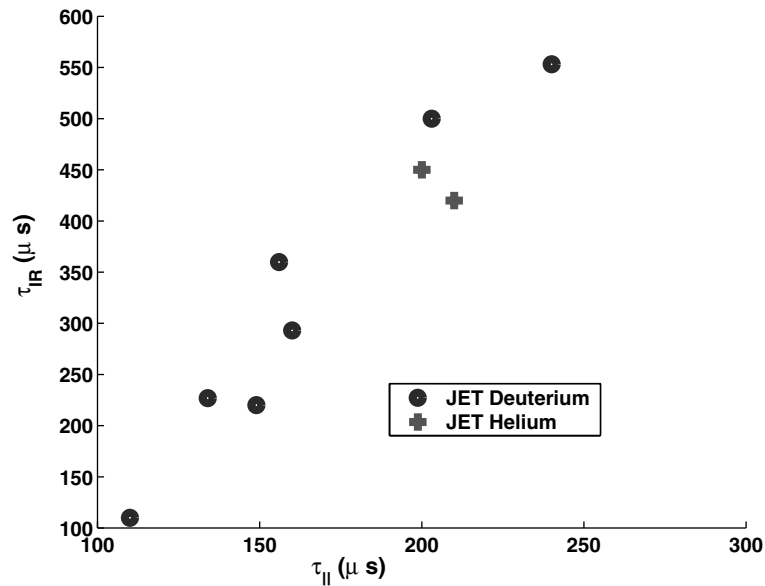


Fig. 4. Correlation of the ELM rise time and the parallel ion flight time in the SOL. The ELM power deposition time varies in the range of 100  $\mu$ s up to 550  $\mu$ s. Values for the ELM power deposition time in JET MKIIGB helium discharges are included.

been gained in JET MKIIGB divertor campaign and are compatible to results reported from ASDEX Upgrade, DIII-D and JT60-U [11,12]:

- The profile broadening during ELMs does not exceed values 1.5 times the inter-ELM profile. Applying this finding to ITER the wetted area becomes  $\sim 5$  m<sup>2</sup> for each leg.
- The power deposition time is believed to follow the ion transport time in the SOL (as shown in Fig. 3) and is therefore assumed to be around 550  $\mu$ s.
- The ratio of the energy released during the ELM crash and arriving on the target plate is around values of 0.6 and is deposited balanced on the inner and outer divertor.

Note, that the peak value of the power deposition within the wetted area is 1.5–2.0 times higher than the averaged value, depending on the exact profile shape. From current measurements at JET it is not clear, if the peak value of the ELM power deposition is added on top of the steady state profile or moved a within a few mm, which then, due to the high gradients of the power deposition profile on target, leads to a reduced temperature rise during the ELM event. Therefore it is assumed, that the distribution of the power over the total averaged wetted area including the peak value is a reasonable estimate.

Based on these findings, an optimistic calculation would assume that 60% of the mid plane energy loss (15 MJ) is deposited balanced on both targets, and that half

of the target load is deposited during a constant rise of the heat flux within a time of 550  $\mu$ s. In this case the thermal load results in  $\sim 29$  MJ m<sup>-2</sup> s<sup>-1/2</sup> (15 MJ  $\times$   $0.6 \times 0.5 \times 0.5 / 5$  m<sup>2</sup> /  $\sqrt{550}$   $\mu$ s  $\times$  1.5). Note, that a constant rising heat flux instead of a constant (not rising) heat flux leads to the 1.5 times higher value for the thermal load for a given fixed integral energy as used in the latter calculation (semi infinite approximation). These values are only valid for the average ELM, whereas single particular larger ELM events still could lead to even higher heat fluxes (material limits are for tungsten melting 40 MJ m<sup>-2</sup> s<sup>-1/2</sup> and for carbon ablation 20 MJ m<sup>-2</sup> s<sup>-1/2</sup>). For a statistical analysis of ELMs in JET see [9].

Complementary, an upper limit for the expected ITER heat load due to type-I ELMs is calculated next; here it is assumed, that all the energy of 15 MJ is deposited within a constant heat flux of 240  $\mu$ s duration on the wetted area (for one leg), leading to a thermal load of  $\sim 200$  MJ m<sup>-2</sup> s<sup>-1/2</sup> (15 MJ / 5 m<sup>2</sup> /  $\sqrt{240}$   $\mu$ s).

Both values indicate, that type-I ELMs in ITER may be in the range or well above the ablation limit for carbon or melting for tungsten. Extrapolation of present results for ITER ranges from being unacceptable from the divertor life time point of view to being marginally acceptable. Experiments are necessary to understand which is the physics mechanism (pedestal collisionality or parallel SOL energy transport). Such a physics based scaling will provide a more realistic (within smaller error bars) extrapolation of type-I ELM energy load to ITER.

## 5. Conclusions

Using a fast 2D IR system in the ITER like JET MKIIGB divertor, ELMy H-Mode discharges have been investigated with particular focus on SOL transport by type-I ELMs. The influence of surface layers has been taken into account using the THEODOR code for heat flux calculations. It is found, that the energy deposition on the inner and outer divertor is fairly balanced whereas the inter-ELM deposition is governed by the outer divertor. The rise time of the temperature on the outer target was analysed for type-I ELMy H-Mode discharges and shows a clear correlation to the parallel ion transport time in the SOL. Based on these findings, as well as on further assumptions about the expected ITER pedestal plasma properties, lower and upper limits for the ablation limit during ELMs in the ITER type-I reference scenario have been calculated. These results show, that ITER will operate with type-I ELMs close to or above the material limits, incompatible with a long divertor life time.

## Acknowledgement

This work has been conducted under the European Fusion Development Agreement.

## References

- [1] T. Eich et al., ICPP 2000, Quebec, Canada.
- [2] A. Herrmann et al., Proceedings of the 28th EPS Conference, Madeira, 2001.
- [3] S. Clement et al., J. Nucl. Mater. 266–269 (1999) 285.
- [4] A. Herrmann et al., Plasma Phys. Control. Fusion 37 (1995) 17.
- [5] P. Andrew, these Proceedings.
- [6] G. Matthews et al., J. Nucl. Mater. 290–293 (2001) 668.
- [7] A.W. Leonard, J. Nucl. Mater. 266–269 (1999) 109.
- [8] A. Herrmann et al., these Proceedings.
- [9] A. Loarte et al., these Proceedings.
- [10] E. Gauthier et al., Proceedings of the 24th EPS Conference, Berchtesgaden, 1997.
- [11] C.J. Lasnier, J. Nucl. Mater. 290–293 (2001) 1093.
- [12] K. Itami, J. Nucl. Mater. 220–222 (1994) 203.